OPEN ACCESS

University of BRISTOL

Coope, T. S., Wass, D. F., Trask, R. S., & Bond, I. P. (2014). Metal Triflates as Catalytic Curing Agents in Self-Healing Fibre Reinforced Polymer Composite Materials. Macromolecular Materials & Engineering, 299(2), 208-218. 10.1002/mame.201300026

Link to published version (if available):
10.1002/mame.201300026

Link to publication record in Explore Bristol Research
PDF-document

University of Bristol - Explore Bristol Research

General rights

This document is made available in accordance with publisher policies. Please cite only the published version using the reference above. Full terms of use are available:
http://www.bristol.ac.uk/pure/about/ebr-terms.html

Take down policy

Explore Bristol Research is a digital archive and the intention is that deposited content should not be removed. However, if you believe that this version of the work breaches copyright law please contact open-access@bristol.ac.uk and include the following information in your message:

• Your contact details
• Bibliographic details for the item, including a URL
• An outline of the nature of the complaint

On receipt of your message the Open Access Team will immediately investigate your claim, make an initial judgement of the validity of the claim and, where appropriate, withdraw the item in question from public view.

((please add journal code and manuscript number, e.g., DOI: 10.1002/macp.201100001))

Article type: Full Paper

Metal Triflates as Catalytic Curing Agents in Self-Healing Fibre Reinforced Composites

Tim S. Coope, Duncan F. Wass, Richard S. Trask and Ian P. Bond*

T. S. Coope, Dr. R. S. Trask, Prof. I. P. Bond
Advanced Composites Centre for Innovation and Science (ACCIS)
Department of Aerospace Engineering
University of Bristol
Queen's Building, University Walk, Bristol, BS8 1TR, UK
E-mail: I.P.Bond@bristol.ac.uk

Prof. D. F. Wass
School of Chemistry
University of Bristol
Cantock's Close, Bristol, BS8 1TS, UK

A self-healing, high performance, fibre reinforced polymer (FRP) composite material is demonstrated by employing a Lewis acid-catalysed epoxy self-healing agent (SHA) within a laminate manufactured using existing industrial methods. Thermal cure analysis and mechanical testing is employed to characterise the self-healed polymer. A bio-inspired series of vascules incorporated into an FRP composite material facilitates the delivery of self-healing agents to exposed fractured crack planes. Healing is effected by ring-opening polymerisation (ROP) of an epoxy resin using novel metal triflate catalysts injected after Mode I crack opening displacement. Strong adhesive compatibility with the host matrix confers full recovery of mechanical properties (>99% healing).

1. Introduction

Lightweight structures for transport sectors are becoming increasingly prevalent to improve energy efficiency, reduce fuel consumption, increase range, sustain current costs and incorporate sustainable materials.[1-4] The aerospace and automotive industries have led the development and implementation of lightweight fibre reinforced polymer (FRP) materials over the past few years, changing the design envelope to implement new materials[5] and incorporate novel technologies.[6]

As with any relatively 'new' material there are certain design challenges to meet pre-existing operating parameters.[7] Conservative design philosophies for FRP materials are traditionally applied to prevent propagation of any sub-surface structural micro-cracking, which can significantly limit the inherent lightweight nature of such a material. Incorporating a self-healing system capable of restoring mechanical efficiency after damage formation has the potential to reduce maintenance and inspection costs (i.e. non-destructive testing (NDT)) and eliminate challenging, costly and complicated repairs to ultimately realise lighter composite structures.

Micro-cracking in FRP materials can ultimately lead to catastrophic failure by rapid propagation throughout the laminated structure. For example, this damage can occur between stacked laminae, manifest itself as fibre-resin interfacial debonding or arise from manufacturing defects, causing stress concentrations which lead to the onset of premature component failure.[8] In this research the focus has been on the implementation of previously developed self-healing agents by Coope *et al.*,[9] to achieve a self-healing FRP material using typical industrial composite manufacturing techniques. This has the potential to address the issues of internal damage highlighted above and prolong the useful life of materials currently difficult and expensive to repair or recycle through traditional methods.[10]

A bio-inspired vascule approach[11] to self-healing in high performance thermoset composite materials has been extensively researched by Bond, Trask and co-workers over the past 10

years, primarily due to the integration challenges and volume limitations of microcapsule-based systems. Hollow glass fibres (HGFs)[12-16] and microvascular channels[17-20] have successfully demonstrated reliable methods for self-healing agent (SHA) delivery to damaged areas through multiple mixed-mode testing. Norris *et al.* have further developed this concept with the stimuli triggered delivery of a pre-mixed commercial epoxy SHA into an aerospace grade composite material, when subject to low energy impact damage, to recover compression after impact (CAI) strength.[21-23]

As previously discussed,[9] the SHAs implemented in this study offer significant improvements over alternative well documented self-healing systems, for example those employing Grubbs' catalyst,[24] polydimethylsiloxane (PDMS)/di-*n*-butyltin dilaurate (DBTL)[25] and epoxy/maleimide.[26] These improvements include host matrix compatibility, catalytic activity under mild conditions, relatively low cost and toxicity, high stability, commercial availability and system tailorability. In this study, we have further developed the solid phase scandium(III) triflate-epoxy system and also considered other similar metal triflate catalysts to initiate epoxide ring-opening polymerisation (ROP).

Initially, the thermal cure and mechanical properties were assessed to establish the most suitable polymer-solvent formulation for achieving a significant recovery of material properties in FRP epoxy-based composite materials. Ultimately, this demonstrated the system's potential and tailorability as SHA can be successfully delivered by various means, including microvascular networks, HGFs or microcapsules.

Herein, is a demonstration of a self-healing FRP composite material using a double cantilever beam (DCB) coupon specimen geometry, facilitated by the delivery of novel epoxy-metal triflate SHAs via embedded microvascular channels **(Scheme 1)**. The focus of this research was a 'proof of concept' study for fracture repair in FRP test specimens using conventional industrial composite material manufacturing techniques and the aforementioned novel SHAs. As reported below, results have shown a significant recovery of fracture toughness (>99%)

that matches the initial fracture mechanism of the host FRP material and an ability to create a repair with superior toughness than the original host polymer matrix material.

2. Experimental Section

Materials:

Ethyl phenylacetate (EPA), diethylenetriamine (DETA, $(NH_2CH_2CH_2)_2NH$), scandium(III) triflate ($Sc(OTf)_3$), aluminium(III) triflate ($Al(OTf)_3$) and copper(II) triflate ($Cu(OTf)_2$) were purchased from Sigma-Aldrich and used as received. EPON 828 was purchased from Polysciences, Inc.. E-glass/epoxy preimpregnated tape was purchased from Hexcel.

Differential Scanning Calorimetry (DSC):

Samples for the DSC experiments were prepared by mixing catalyst ($Sc(OTf)_3$, $Al(OTf)_3$ or $Cu(OTf)_2$) at the prescribed loading with EPON 828 and EPA solvent. The following wt% of EPA was added to EPON 828; 0 wt% (EPON), 10 wt% (E10) or 25 wt% (E25). The solution was thoroughly mixed at ambient temperature and quickly transferred (approximately 10 mg) to aluminium Tzero hermetic pans. A TA Instruments Q200 DSC was used to study non-isothermal curing via dynamic scans. Samples were heated from 0 to 250 °C at a heating rate of 10 °C/min under a flow rate of 50 mL/min of nitrogen as the purge gas. Glass transition temperatures (T_g) were obtained using a temperature range of -30 to 100 °C at a heating rate of 3 °C/min under a flow rate of 50 mL/min of nitrogen as the purge gas.

Fibre-Reinforced Polymer (FRP) Composite Material Manufacture:

E-glass/epoxy (Hexply 913, Hexcel Composites) unidirectional (UD) plates (300 mm x 220 mm x 3.8 mm) were manufactured using hand lay-up (28 ply). Cure was undertaken according to the manufacturer's recommendations of 125 °C for 1 hour and a pressure of 700 kPa. Stainless steel wire (ca. 0.5 mm in diameter) pre-coated with PTFE release agent was

placed parallel to the fibre direction in pre-cut 0.5 mm channels (equal to the thickness of 4 plies) centred on the mid-plane.

Release film (15 μm thickness) was placed from the laminate edge to 25 mm before the start of the vascules. Cured composite plates were cut into DCB coupon specimens using a water-cooled diamond grit saw (195 mm x 20 mm x 3.8 mm). Piano hinges were bonded in place using Hexcel Redux 810 adhesive onto grit-blasted surfaces as preparation for mechanical testing.

Fibre-Reinforced Polymer (FRP) Composite Material Testing:

An Instron 3343 fitted with a 1kN load cell was used to initiate and propagate Mode I crack opening. Double cantilever beam (DCB) E-glass composite test specimens fixed via attached piano hinges **(Scheme 1)** were loaded at a displacement rate of 2 mm/min in accordance with ASTM 5528-01.[27] Cracks were propagated for 75 mm from the point of initiation and crack length recorded with a video camera.

Specimens were healed after initial fracture using the prescribed healing agent, delivery method and cure temperature **(Table 1)**. SHAs were delivered via the edge-located vascules using 26 gauge hypodermic needles. Healed specimens were re-tested as outlined above for initial fracture.

3. Results and Discussion

3.1. Differential Scanning Calorimetry (DSC)

The catalytic activity of scandium(III) triflate ($Sc(OTf)_3$) with an oligomeric DGEBA epoxy resin (EPON 828) was investigated using differential scanning calorimetry (DSC). A number of variables were identified for analysis such as solvent quantity [ethyl phenylacetate (EPA)] blended with EPON 828 resin, catalyst loading and catalyst type.

Dynamic experiments in the range 0-250 °C at a rate of 10 °C/min used an initial medium (M) catalyst loading [3.125 pph]. Cure onset temperatures for ROP of EPON 828 containing 10 wt% EPA (E10) and 25 wt% EPA (E25) gave values of 34.6 °C and 49.8 °C respectively, a significant reduction when compared with the solvent free EPON 828 derivative (81.6 °C) **(Figure 1)**. Modifying the catalyst concentration to higher (H) [6.25 pph] and lower (L) [1.5625 pph] loadings confirmed predictions of a retrospective decrease (27.9 °C) and increase (79.3 °C) of cure onset temperature for E10 Sc derivatives.

In addition, dynamic scans of isothermal cured polymer were undertaken after their respective healing duration (i.e. 24 hr: 45/80 °C; 7 days: RT) to determine glass transition temperatures (T_g). These conditions were investigated due to the comparison to commercially available epoxy systems typically used in composite material manufacture and repair. Furthermore, this experimental data highlighted complete cure after these isothermal cure durations. The T_g values are summarised in **Table 2**.

Alternative metal triflates such as aluminium(III) triflate ($Al(OTf)_3$) and copper(II) triflate ($Cu(OTf)_2$) were also investigated as commercially readily available and lower cost alternatives to $Sc(OTf)_3$. Experiments containing $Al(OTf)_3$ and $Cu(OTf)_2$ with a E25 monomer-solvent solution resulted in similar cure onset temperatures to $Sc(OTf)_3$ for all three catalyst loadings. However, a reduction in solvent quantity (i.e. from E25 to E10) reduces the activity of $Al(OTf)_3$ and more significantly for $Cu(OTf)_2$ **(Table 3)**. This is attributed to catalyst solubility in EPA solvent. Therefore, $Sc(OTf)_3$ and $Al(OTf)_3$ catalysts were pursued as SHAs in this study. These results are further summarised in the Supporting Information.

This DSC study was carried out to identify the most reliable low temperature or autonomous ROP-based self-healing system by considering the catalytic activity of metal triflates and EPON 828 with respect to solvent and catalyst loadings. Solvent inclusion in a non-solvated system has a significant effect on achieving low temperature curing. Increasing solvent concentration further, for example, from 25 wt% to 50 wt% dilutes this effect due to increased

mobility and reduced contact of active sites in the reagent mixture. Furthermore, increasing catalyst loading also reduces the onset temperature for polymerisation where catalyst solubility is permitted.

3.2. Fracture Testing

Self-healing performance was assessed in an FRP material using a microvascular double cantilever beam (DCB) test specimen arrangement as developed by Norris *et al*..[19] This method is based on the ASTM D5528-01 standard for Mode I crack opening displacement of FRP composite materials,[27] a unidirectional (UD) glass fibre reinforced epoxy composite (HexPly 913, Hexcel Composites) was manufactured with two 0.5 mm longitudinal vascules along the central mid-plane to facilitate external self-healing agent injection **(Figure 2)**. Mode I crack opening displacement has been thoroughly investigated to provide successful crack-microvascule interconnectivity to allow SHAs to wet out the crack planes and re-bond fractured surfaces.[19,20] Test specimens were initially fractured, unloaded from the test machine, allowed to heal and subsequently re-tested to failure following the same protocol. Mode I strain energy release rate, G_{IC}, values were calculated from load (P), displacement (δ), delamination length (a) and specimen width (b) values using the modified beam theory (MBT) method **(Equation 1)**. As the beam is not perfectly built-in, rotation may occur at the delamination front; therefore a correction factor, Δ, is incorporated which treats the DCB specimen as if it contained a slightly longer delamination ($a + |\Delta|$). Δ was calculated experimentally by generating a least squares plot of the cube root of compliance, $C^{1/3}$, as a function of delamination length. [27] Healing efficiencies (ζ) were calculated for each individual test specimen using the initial (P_{Initial}) and healed (P_{Healed}) fracture load values **(Equation 2)** and crack initiation fracture toughness values in terms of the strain energy release rate (G_{IC}) **(Equation 3)**. The data presented here corresponds to average data points obtained from at least 5 replicates.

$$G_{Ic} = 3P\delta / 2b(a + |\Delta|) \quad (1)$$

$$\xi_{LOAD} = P_{Healed} / P_{Initial} \quad (2)$$

$$\xi_{G_{IC}} = G_{IC\,Healed} / G_{IC\,Initial} \quad (3)$$

Mechanical testing of the cured bulk self-healed polymer was carried out using the previously documented modified TDCB test specimen arrangement to initially identify a suitable polymer formulation to achieve the required self-healing functionality in FRP composite materials.[9,28] Inclusion of a higher wt% of EPA solvent resulted in a ductile failure mechanism, an important parameter when healing such an inherently brittle host material. These results are summarised in the Supporting Information. Specimen derivatives including SHA reagent combinations, healing conditions and delivery methods used in the DCB testing are outlined in **Table 1**. A summary of strain energy release rates (G_{IC}) with respect to crack length (a) is outlined in **Figures 3 and 4**.

3.2.1. Benchmark Commercial Healing System

A commercially available epoxy-amine thermoset, consisting of EPON 828 and diethylenetriamine (E25 DETA), was selected as a benchmark resin system for this study. EPA solvent (25 pph) was added to reduce viscosity and aid resin infusion via the microvascular channels.[21] Initial fracture toughness testing of five baseline FRP specimens at a displacement rate of 2 mm/min resulted in progressive crack propagation along the mid-plane at an average load of 27.2 N; a failure mode typical of Mode I loaded UD test specimens. An average strain energy release rate (G_{IC}) value of 218 J/m^2 for delamination initiation was derived from these results.

The fractured test specimens were subsequently prepared for healing by applying one-sided adhesive release tape (63 micron thickness), 1.5 mm across the crack plane from the perimeter

edges of fractured surfaces, and areas to be non-bonded (i.e. the starter pre-crack region of the specimen). This is primarily to constrain the injected SHA on the crack plane and prevent leaching during cure. Furthermore, the void (126 micron thickness) created between the fractured surfaces, by the presence of the tape, is representative of that formed when internal barely visible impact damage (BVID) is generated in FRP composite materials after an impact. This feature has recently been characterised and investigated using micro-CT.[29]

The E25 DETA pre-mixed SHA was introduced via the edge-located vascules and left to cure in accordance with the manufacturer's specifications (7 days, 25 °C). The SHA was allowed to wet out the crack plane with no external intervention to influence SHA distribution on the fracture surfaces. This factor is critical in trying to replicate the likely SHA delivery mechanism in large-scale FRP components.

Healed specimens achieved an average recovery of greater than 95% initial fracture toughness and 86% peak load. The average healed failure load value corresponded to 23.5 N.

3.2.2. Low Temperature (45 °C) Healing System

A low temperature healing cure cycle consisting of 45 °C for 24 hours was selected as being easily achievable during existing maintenance schedules for a FRP composite structure. Furthermore, results from DSC thermal cure analysis highlighted that healing with a medium catalyst loading (M) [3.125 pph] is achievable at temperatures marginally above ambient. In addition, the effect of different quantities of EPA solvent on the ability to infuse SHA and the resulting polymer and mechanical performance was investigated by considering E10 and E25 monomer solutions.

$Sc(OTf)_3$ [3.125 pph] combined with E10 monomer (E10 Sc (M)) achieved a healed average recovery of greater than 119% initial fracture toughness and 104% peak load. Therefore, the material properties of the resulting healed polymer are at least equal to the material properties

of the host matrix. If damage were to occur in the same region it is likely that the crack would deviate away from the healed region and propagate through the existing host matrix. Due to the small quantity of solvent present, the resulting polymer is inherently brittle, similar to most cured epoxide materials, resulting in a 'sawtooth' load-displacement plot (**Figure 5**). This behaviour is supported using microscopic techniques in **Section 2.3**.

In comparison, mechanical testing of the same polymer formulation using E25 monomer (E25 Sc (M)) revealed a very different fracture pattern. Due to the high boiling point (229 °C) of the EPA solvent, it effectively acts as a plasticiser in the healed polymer. Therefore, a ductile load-displacement plot is observed which is similar to the initial fracture response of the host material **(Figure 6)**. This also results in an average of 26% and 81% increase in peak load and fracture toughness healing efficiencies, respectively, when compared to the lower solvated derivative, E10 Sc (M) **(Figure 7)**. Additionally, in this study, environmental testing has confirmed this as not being a transitional state.

To consider the end-user usability of such a system, experimentation into the catalyst loading was sought to establish if healing efficiencies could be maintained at higher (H) [6.25 pph] and lower (L) [1.5625 pph] catalyst concentrations. Therefore, test specimens were healed with double and half catalyst concentrations of the E25 Sc (M) derivative. From five test replicates, an increase of 46% healed peak load and 152% healed fracture toughness was observed when doubling catalyst concentration (E25 Sc (H)). Subsequently, test specimens (5) healed with a reduced catalyst concentration (E25 Sc (L)) achieved comparable results to E25 Sc (M), with a 1% healed load decrease and a 22% healed fracture toughness decrease. When taking into account the standard deviation of these values it can be concluded that a reduction in catalyst concentration can achieve comparable healing efficiencies at the point of delamination initiation. Therefore, a healthy reserve factor could be applied to E25 Sc (M) in an industrial application to achieve a minimum healing efficiency value in line with E25 Sc (L) test specimen results.

As confirmed from the DSC results, $Al(OTf)_3$ has a similar reactivity although a slight reduction in solubility in comparison to $Sc(OTf)_3$. Therefore, E10 and E25 $Al(OTf)_3$ 3.125 pph (E10 Al (M), E25 Al (M)) were employed as healing agents to establish if similar mechanical properties could be achieved by using this significantly more economically viable catalyst.

From a total of five test replicates, E10 Al (M) specimens achieved a marginal decrease in healing efficiency for fracture toughness (-10%) and peak load (-6%) when compared to $Sc(OTf)_3$. Similarly, E25 Al (M) specimens achieved a decrease in healing efficiency for fracture toughness (-59%) and peak load (-19%). Therefore, additional catalyst could be employed to achieve higher healing efficiencies and improved reactivity than $Sc(OTf)_3$, but at a much lower cost.

3.2.3. High Temperature (80 °C) Healing System

Curing of $Sc(OTf)_3$ healed specimens at a higher temperature was investigated to establish if significant improvements in healing efficiencies could be achieved. The most promising formulations (E10 Sc (M) and E25 Sc (M)) from the low temperature study were healed at 80 °C for 24 hours and subsequently re-tested at ambient temperature. From a total of five test replicates, E10 Sc (M) specimens achieved a negligible change in healing efficiency for fracture toughness (-7%) and peak load (+2%) when compared to the lower temperature counterpart.

In comparison, healed E25 Sc (M) specimens achieved on average a 29% and 106% increase in peak load and fracture toughness healing efficiencies. Therefore, the average healed peak load value (44.2 N) was significantly higher than the initial fracture peak load value (27.8 N), resulting in an overall healing efficiency of 159%.

3.2.4. Ambient Temperature Healing System

To achieve an autonomous self-healing composite material, test specimens were infused with a pre-mixed solution and left to cure at ambient temperature (RT) for 7 days. This healing scheme is typical of ambient temperature cured epoxy systems. The derivatives demonstrated in this study include E10 Sc (M), E25 Sc (M) and E25 Sc (H) as these were highlighted as the best overall analogues in the 45 °C / 24 hour healing scheme. DSC analysis of the resultant SHP showed complete cure in this time period.

Firstly, E25 Sc (M) was evaluated, giving a load healing efficiency of 113% and a fracture toughness healing efficiency of 121%. Comparing these values with the 45 °C cured derivative reveals a 17% reduction in load healing efficiency and a 79% reduction in fracture toughness healing efficiency. Furthermore, these ambient temperature results are comparable with E25 Al (M) healed at 45 °C for 24 hours. On increasing catalyst concentrations the maximum load (127%) and fracture toughness (185%) healing efficiencies become comparable to E25 Sc (L) healed at 45 °C for 24 hours with values of 129% and 178%, respectively.

Lastly, evaluating E10 Sc (M) healed at ambient temperature reveals a decrease in healing efficiency of 32% for maximum load (72%) and a decrease in healing efficiency of 35% for fracture toughness (84%). Therefore, it was observed that to maintain healing efficiencies close to the fracture toughness of the host matrix at ambient temperature, a higher quantity of solvent (E25) is required. This is attributed to reagent migration within the solvated healing polymer during cure.

The complete data set for the fracture toughness of all test specimen derivatives are listed in **Table 4**.

3.2.5. Autonomous Delivery System

An autonomous delivery system was investigated to demonstrate self-healing functionality where separate solutions of $Sc(OTf)_3$-EPA and EPON 828-EPA were introduced via parallel microvascular networks (AUTO - AUTO E25 Sc (M)). The total solvent and catalyst loading was analogous to E25 Sc (M) and cured at 45 °C for 48 hours. A longer cure time was prescribed to account for catalyst infusion throughout the monomer solution. Ultimately, if this were to occur in a pressurised system the rate of autonomous mixing would greatly increase and would, therefore, be comparable to derivatives healed using a pre-mixed solution.

From five test replicates, healing efficiencies for load and fracture toughness at delamination initiation were 100% and 88%, respectively. However, as the extension was increased from this point the load carrying capability also increased until a reduction in maximum load was observed at ~20 mm extension. Therefore, AUTO specimens showed a higher degree of ductility to achieve a maximum load comparable to the host matrix at >100% increase in extension. Therefore, the fracture toughness was considerably higher (2-3 times) at the point of maximum load than observed for pre-mixed samples.

3.3. Microscopy

Fractured crack planes from healed E25 and E10 specimens were imaged using a Zeiss EVO MA 25 scanning electron microscope (SEM). DCB specimens were clamped open and mounted in the large chamber under variable pressure to observe the fractured surfaces. Fracture surface evaluation revealed a cohesive failure in both sample sets, highlighting strong adhesive bonding between the self-healed polymer (SHP) and the exposed untreated crack plane. **Figure 8** shows hackle marks parallel to the line of propagation running in bands across the test specimen width in E10 test specimens. These fracture lines are present at the point at which a significant load drop occurs and form part of the energy dissipation

mechanism to prevent further propagation in the extension loaded test specimen. This is attributed to the brittle nature of this low solvated SHA polymer. The initial fracture surface is annotated for comparison with the SHP, representing a fracture plane with loose fibres and debris, which is typical of pre-impregnated manufactured composite materials tested under Mode I.

Conversely, the micrograph from an E25 specimen **(Figure 9)** confirms the ductile failure as observed in **Figure 6**. This is identified by ductile-hackle features around loose glass fibres and the SHP and is primarily caused by the solvated polymer inducing greater plasticity as it is peeled apart during testing.

3.4. Research Focus and Summary

The previously demonstrated DGEBA-EPA + scandium triflate catalyst self-healing system was further developed and refined to facilitate self-healing in high performance FRP composite materials. By incorporating bio-inspired vascular channels into the material, autonomous delivery of healing agent was possible without having a detrimental effect on the host material mechanical properties.

Evaluating the mechanical properties for solvated metal triflate-initiated epoxide polymers was sought by using a FRP composite material DCB geometry. In total, two EPA solvent concentrations, three healing temperatures, three catalyst loadings, two metal triflate catalysts and two delivery methods were investigated in order to achieve high performance healing using a low temperature-short healing time protocol. Solvent concentration had the greatest influence with regards to the resultant fracture of the healed polymer. Although a cohesive failure in all specimens was observed, the inclusion of a low solvent quantity (i.e. E10 derivatives) facilitated a brittle fracture whereas E25 derivatives with more solvent failed in a ductile manner, similar to the host material behaviour. Both solvated derivatives achieved comparable peak load values at the point of delamination initiation.

Achieving self-healing in FRP composite materials at ambient temperature, restoring mechanical properties comparable to the host matrix, was the predominant focus for this study. Similar to the findings for test specimens healed at low temperature, there was a direct correlation between solvent quantity and fracture pattern and also between catalyst loading and healing efficiencies. This is attributed to the solvent acting as a plasticiser, enhancing ductility and facilitating SHA migration between fracture surfaces to achieve high cross-linking density from metal triflate-initiated epoxide sites. Healing at a higher temperature does not induce a significant increase in healing performance over specimens healed at low or ambient temperatures when considering the extra energy required.

E25 Sc (M) was highlighted as the best overall specimen derivative to achieve reliable healing performance equal or greater than the host material mechanical properties. Therefore, a medium catalyst loading [3.125 pph] was chosen as a representative value to evaluate $Al(OTf)_3$ as a catalytic curing agent for FRP composite materials. This also represented a cost effective, active quantity capable of curing at low and ambient temperatures. Modified catalyst loadings were limited to E25 Sc derivatives cured at 45 °C and ambient temperatures due to reduced solubility of $Al(OTf)_3$ in EPA solvent. Furthermore, healing temperatures were limited to 45 °C, 80 °C and ambient temperature in line with previously investigated self-healing systems and the aim of this study, i.e. to maintain minimum external energy input for healing to occur. In addition, the resultant failure loads for healed specimens correlated well with the T_g values obtained from DSC thermal analysis. Higher failure loads were achieved from SHPs with higher T_g values and vice versa.

4. Conclusion

Aerospace-grade FRP composite materials were self-healed via injection of EPON 828 and Lewis-acid metal triflate catalysts. A 26% minimum healing efficiency increase was observed for implementing these SHAs compared with the commercial-based EPON 828/DETA

system. DCB test specimens were fabricated with 0.5 mm microvascular channels as an integral non-detrimental network for the delivery of SHAs to damaged regions in the material. Test specimen derivatives independently considered monomer-solvent content, healing temperature, catalyst type and catalyst loading.

E25 Sc healed test specimens achieved a minimum healing efficiency of 129% via the injection of a pre-mixed solution at 45 °C, demonstrating full recovery of fracture toughness. Ultimately, autonomous curing was one of the main objectives for this self-healing system. Thus, curing at ambient temperature provided a minimum healing efficiency of 113% for this same system. A modest increase of 30% healing efficiency resulted from healing at 80 °C when compared with healing at low temperature. The highest healing efficiency was achieved by introducing a higher catalyst concentration to E25 Sc cured at 45 °C. This resulted in a 176% load recovery and a 352% fracture toughness recovery. Furthermore, an autonomous delivery method facilitated by infusion of separate $Sc(OTf)_3$-EPA and EPON 828 solutions via parallel vascules achieved a 100% load recovery and 88% fracture toughness at delamination initiation.

Healing a load bearing high performance material remains one of the key challenges in developing and implementing self-healing materials. In this study we have successfully demonstrated high healing efficiencies for fracture toughness recovery at modest raised and ambient temperatures in a FRP composite material manufactured using conventional industrial methods. This research further demonstrates the application and tailorability of the underpinning chemistry of this self-healing system across a variety of delivery systems. Therefore when coupled with structural health monitoring (SHM) systems and a pressurised pumping system it is potentially capable of multiple healing cycles and being truly autonomous in nature.[23]

Acknowledgements: The authors would like to acknowledge the UK Engineering and Physical Sciences Research Council (EPRSC) [EP/G036772/1] and the UK Ministry of Defence/Defence Science and Technology Laboratory for funding this research, the Materials Laboratory at the National Composites Centre (NCC) for use of the SEM and the following individuals, Mr I. K. Chorley and Mr G. D. Wallington, for their assistance in the preparation of the composite laminates.

Received: ((will be filled in by the editorial staff)); Revised: ((will be filled in by the editorial staff)); Published online: (DOI: 10.1002/mame.201300026)

Keywords: bio-inspired; ductile failure; epoxy; ring-opening polymerisation; self-healing

[1] K. Holmberg, P. Andersson, A. Erdemir, *Tribol. Int.* **2012**, *47*, 221.

[2] R. A. Witig, J. Payet, V. Michaud, C. Ludwig, J-A. E. Manson, *Compos. Pt. A – Appl. Sci. Manuf.* **2011**, *42*, 1694.

[3] G. Koronis, A. Silva, M. Fontul, *Compos. Pt. B* **2013**, *44*, 120.

[4] P. D. Mangalgiri, *Bull. Mater. Sci.* ***1999***, *22*, 657.

[5] A. K. Noor, S. L. Venneri, D. B. Paul, M. A. Hopkins, *Comput. Struct*. ***2000***, *74*, 507.

[6] K. Diamanti, C. Soutis, *Prog. Aeronaut. Sci.* ***2010***, *46*, 342.

[7] M. Bannister, *Compos. Pt. A – Appl. Sci. Manuf.* ***2001***, *32*, 901.

[8] W. J. Cantwell, J. Morton, *J. Strain Anal.* ***1992***, *27*, 29.

[9] T. S. Coope, U. F. J. Mayer, D. F. Wass, R. S. Trask, I. P. Bond, *Adv. Funct. Mat.* **2011**, *21*, 4624.

[10] Y. Yang, R. Boom, B. Irion, D-J. van Heerden, P. Kuiper, H. de Wit, *Chem. Eng. Process.* ***2012***, *51*, 53.

[11] R. S. Trask, I. P. Bond, *J. Royal Soc. Interface* **2010**, *7*, 921.

[12] J. W. C. Pang, I. P. Bond, *Compos. Pt. A – Appl. Sci. Manuf.* **2005**, *36*, 183.

[13] J. W. C. Pang, I. P. Bond, *Compos. Sci. Technol.* **2005**, *65*, 1791.

[14] G. Williams, R. Trask, I. Bond, *Compos. Pt. A – Appl. Sci. Manuf.* **2007**, *38*, 1525.

[15] R. S. Trask, G. J. Williams, I. P. Bond, *J. Royal Soc. Interface* **2007**, *4*, 363.

[16] G. J. Williams, I. P. Bond, R. S. Trask, *Compos. Pt. A – Appl. Sci. Manuf.* **2009**, *40*, 1399.

[17] H. R. Williams, R. S. Trask, I. P. Bond, *Smart Mater. Struct.* **2007**, *16*, 1198.

[18] H. R. Williams, R. S. Trask, I. P. Bond, *Compos. Sci. Technol.* **2008**, *68*, 3171.

[19] C. J. Norris, R. S. Trask, I. P. Bond, *Compos. Sci. Technol.* **2011**, *71*, 847.

[20] C. J. Norris, R. S. Trask, I. P. Bond, *Compos. Pt. A – Appl. Sci. Manuf.* **2011**, *42*, 639.

[21] C. J. Norris, G. Meadway, M. O'Sullivan, I. P. Bond, R. S. Trask, *Adv. Funct. Mater.* **2011**, *21*, 3624.

[22] C. J. Norris, I. P. Bond, R. S. Trask, *Compos. Pt. A – Appl. Sci. Manuf.* **2013**, *44*, 78.

[23] C. J. Norris, J. A. P. White, G. McCombe, P. Chatterjee, I. P. Bond, R. S. Trask, *Smart. Mater. Struct.* **2012**, *21*, *doi:10.1088/0964-1726/21/9/094027*

[24] M. R. Kessler, N. R. Sottos, S. R. White, *Compos. Pt. A – Appl. Sci. Manuf.* **2003**, *34*, 743.

[25] S. H. Cho, H. M. Andersson, S. R. White, N. R. Sottos, P. V. Braun, *Adv. Mater.* **2006**, *18*, 997.

[26] S. Billiet, W. Van Camp, X. K. D. Hillewaere, H. Rahier, F. E. Du Prez, *Polymer* **2012**, *53*, 2320.

[27] ASTM International, Test Method Designation: D5528-01

[28] W. Beres, A. K. Koul, R. Thamburaj, *J. Test. Eval.* **1997**, *25*, 536.

[29] G. McCombe, J. Rouse, R. S. Trask, P. J. Withers, I. P. Bond, *Compos. Pt. A – Appl. Sci. Manuf.* **2012**, *43*, 613.

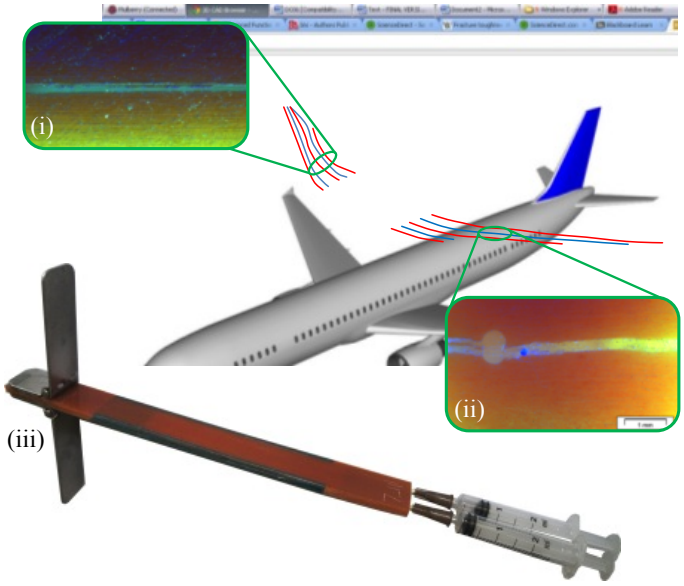

Scheme 1. A schematic of a bio-inspired microvascular self-healing system incorporated into an aerospace structure, representing (i) self-healing between fractured crack planes, (ii) microvascular-fracture plane interconnectivity and (iii) concept demonstration using a FRP composite material DCB coupon specimen.

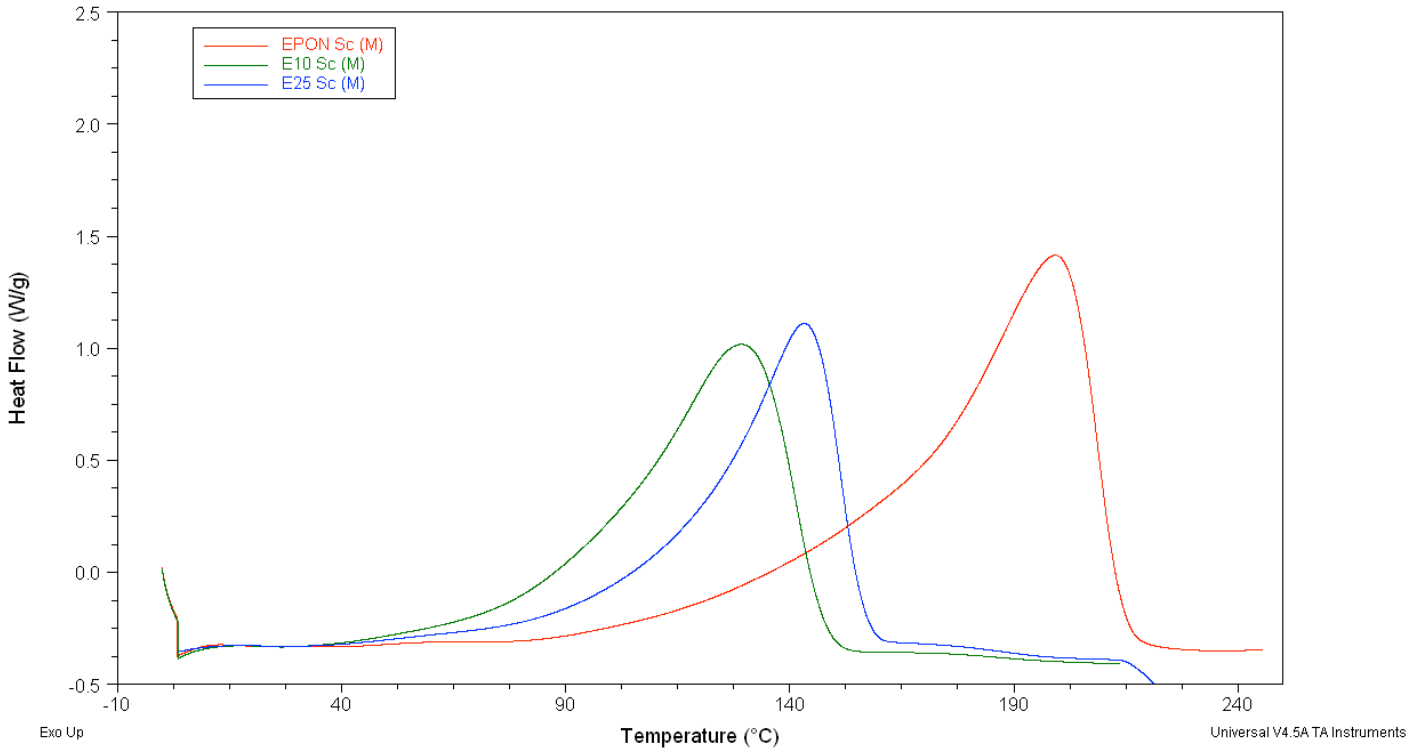

Figure 1. DSC curves for E10 Sc (M), E25 Sc (M) and EPON Sc (M) samples.

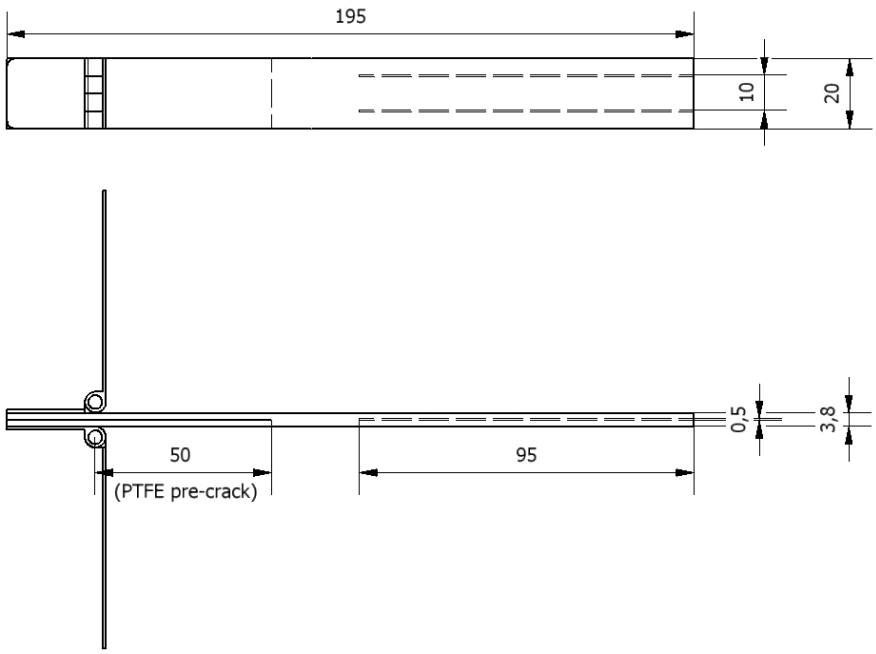

Figure 2. Double cantilever beam (DCB) Mode I specimen geometry. Note: all dimensions in mm; dashed lines represent internal features.

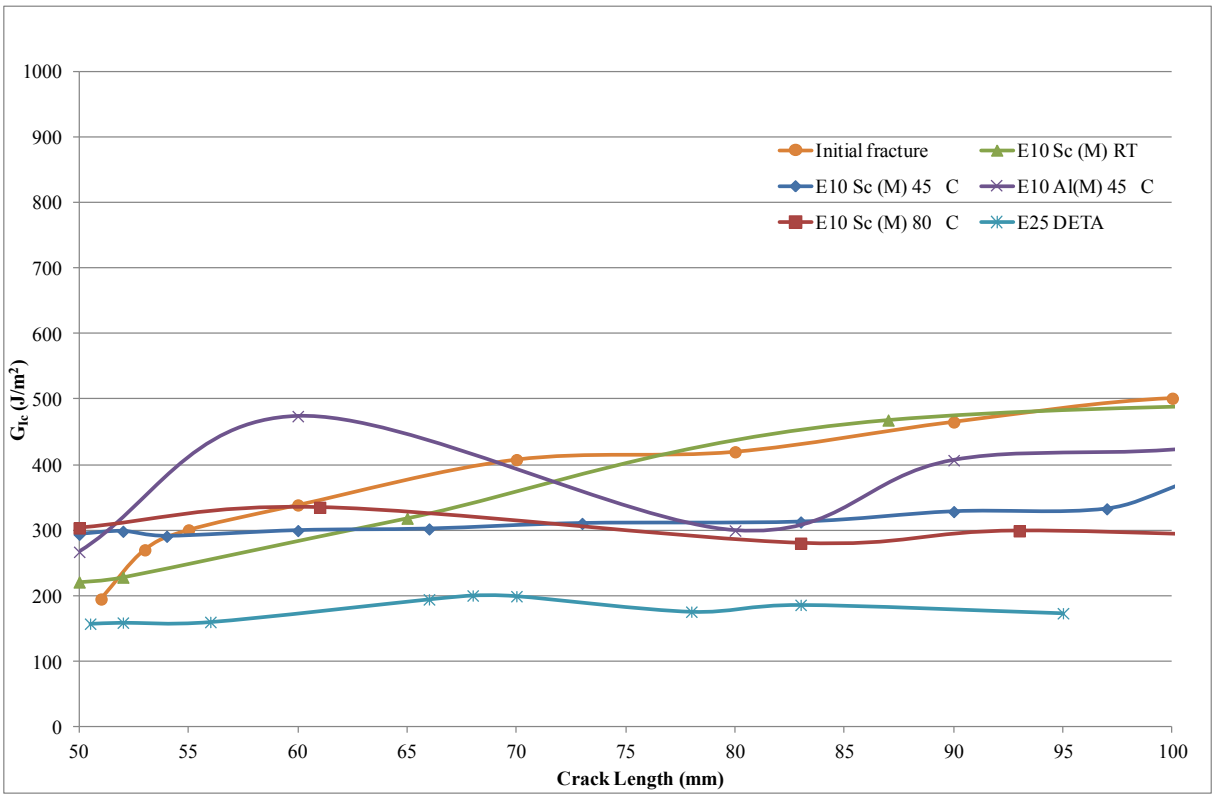

Figure 3. Representative Mode I strain energy release rate (G_{Ic}) data for healed E10 Sc derivatives and E25 DETA.

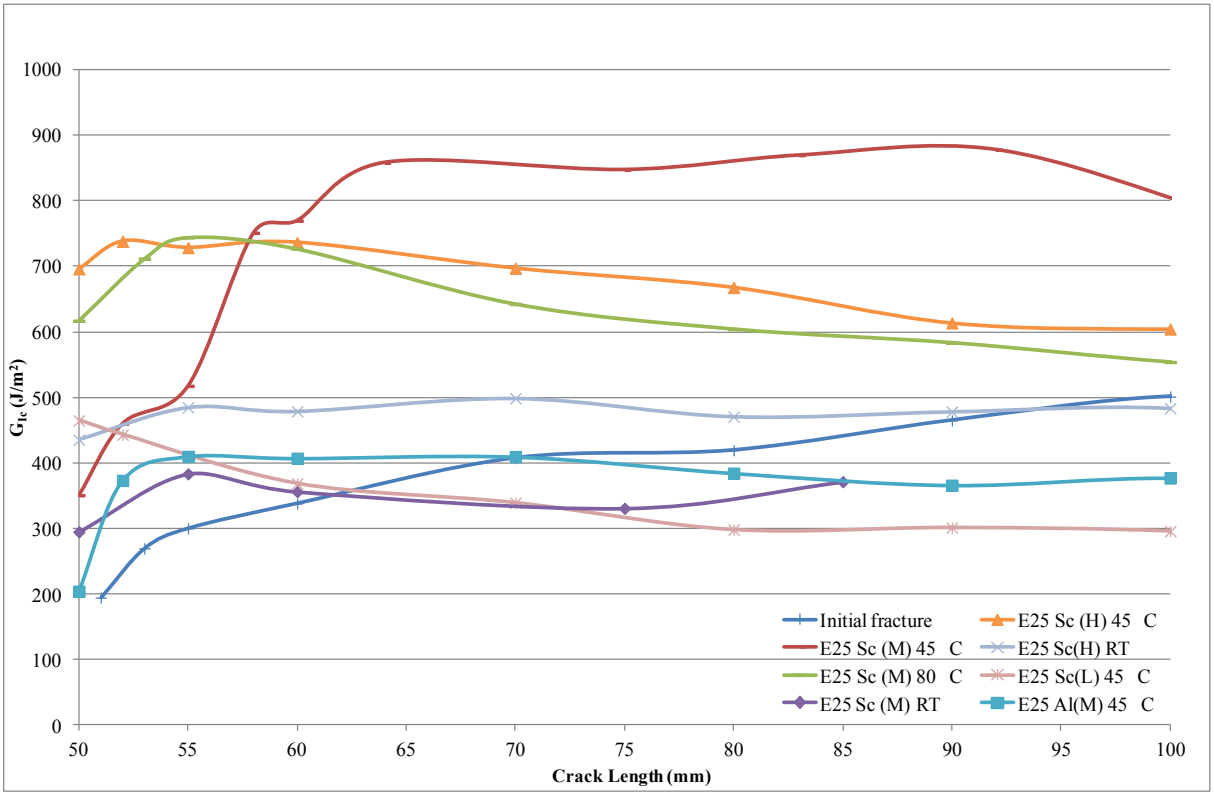

Figure 4. Representative Mode I strain energy release rate (G_{Ic}) data for healed E25 Sc derivatives and E25 Al (M) 45 °C.

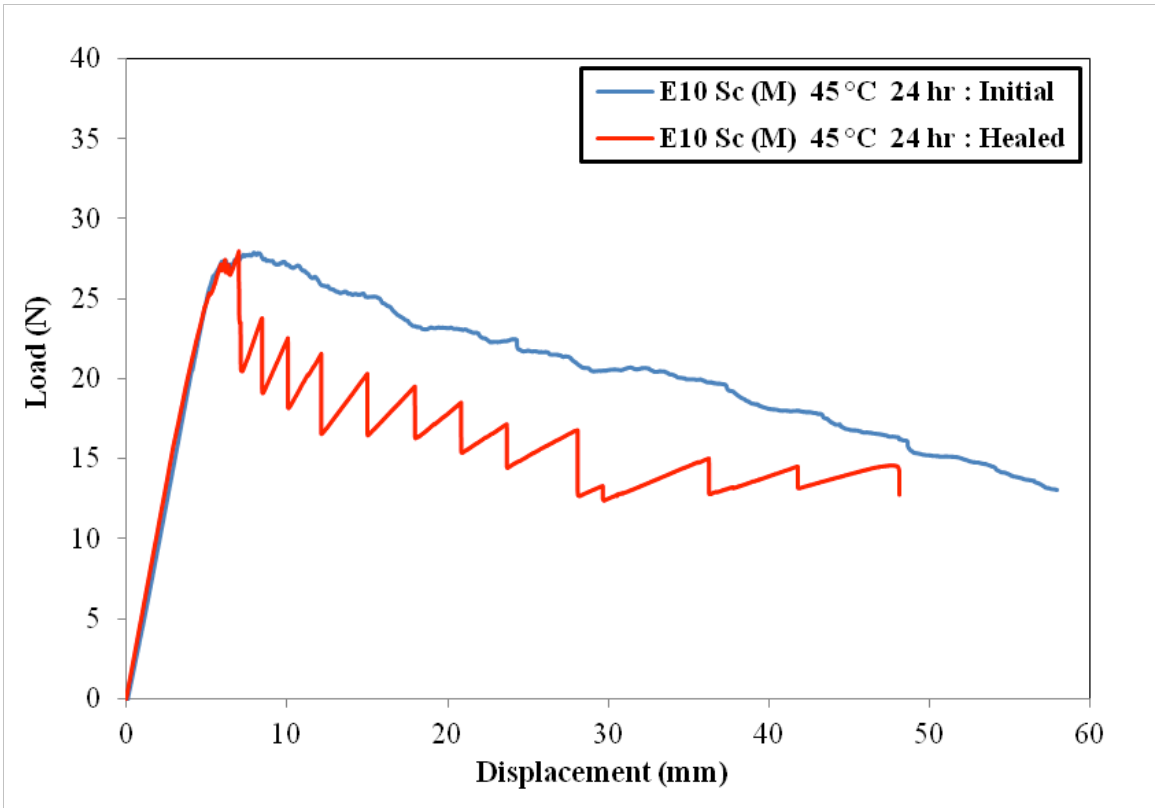

Figure 5. Representative load-displacement curves for E10 Sc (M) DCB test specimens healed at 45 °C for 24 hours.

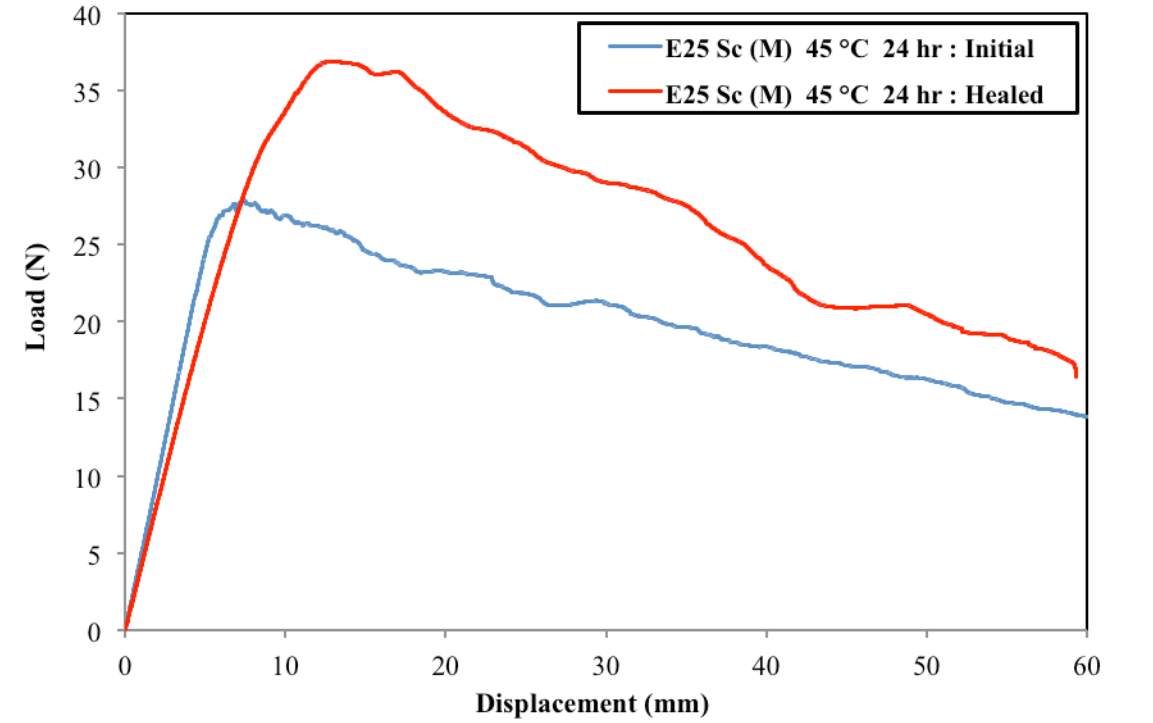

Figure 6. Representative load-displacement curves for E25 Sc (M) DCB test specimens at 45 °C for 24 hours.

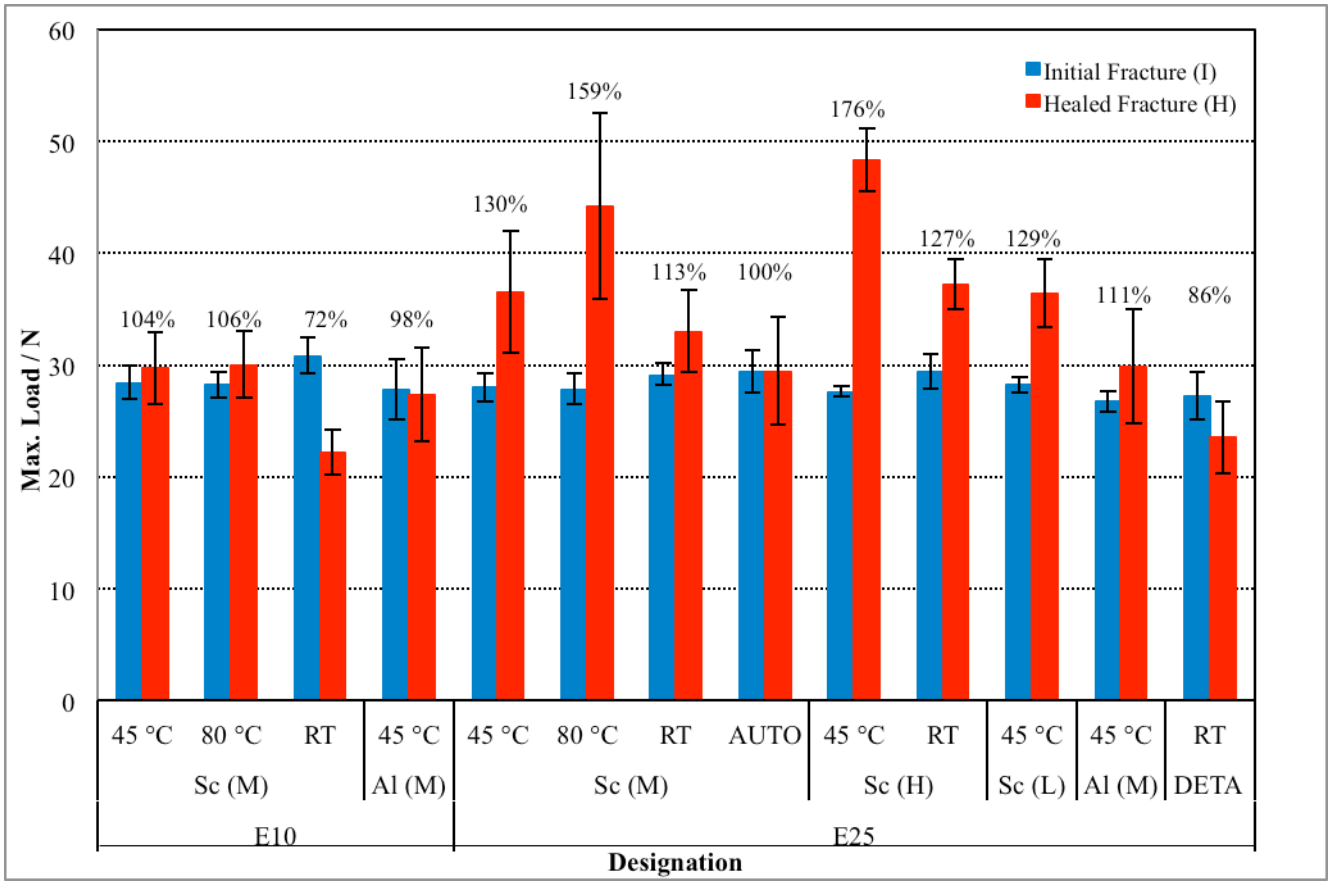

Figure 7. Healing performance for maximum load.

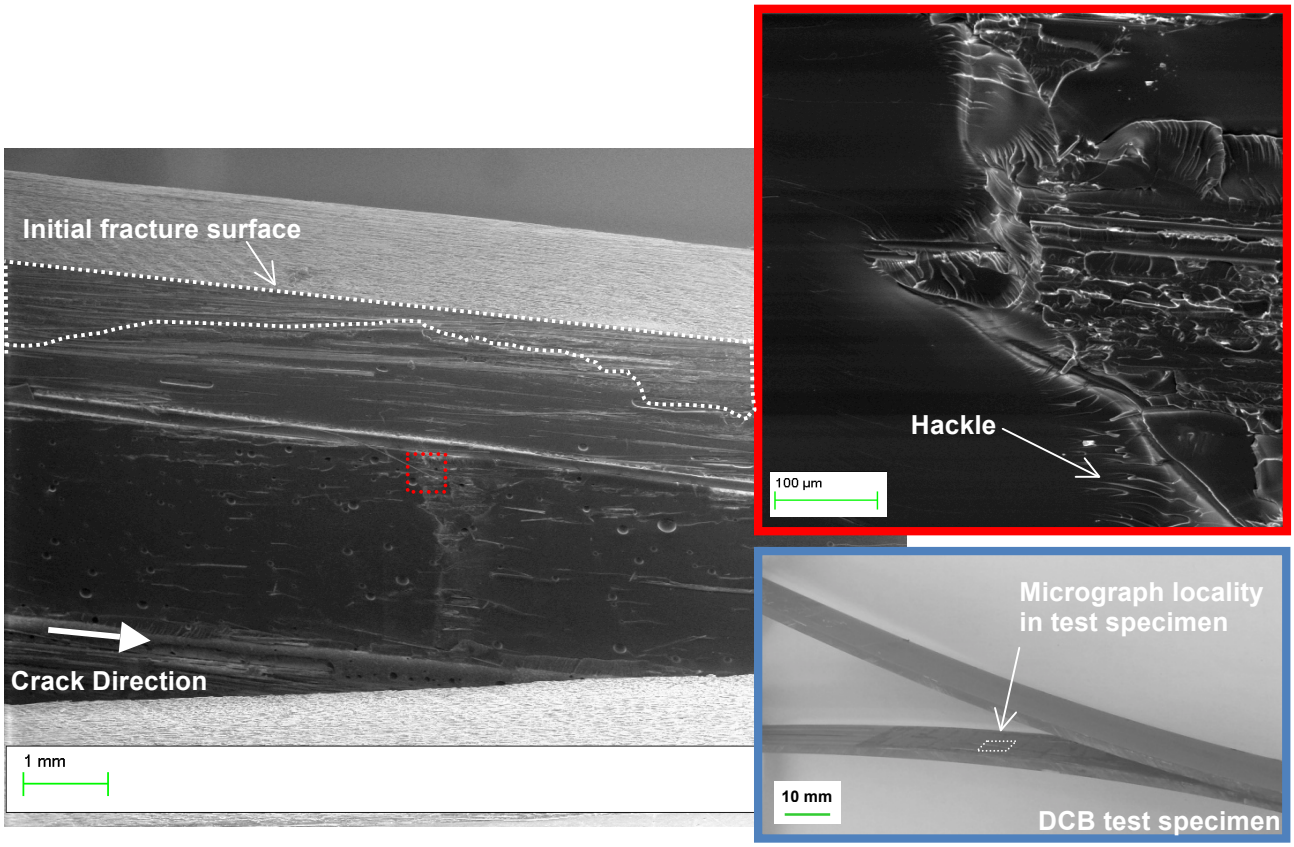

Figure 8. Microscopy investigation of the fracture plane for an E10 Sc (M) healed DCB specimen after re-test. Main image: Scanning electron micrograph (SEM) of the fracture plane. Lower inset image: Macro image of the DCB specimen indicating the position of the SEM image. Upper insert image: SEM of the fracture plane at higher magnification illustrating 'hackle' marks parallel to the line of crack propagation.

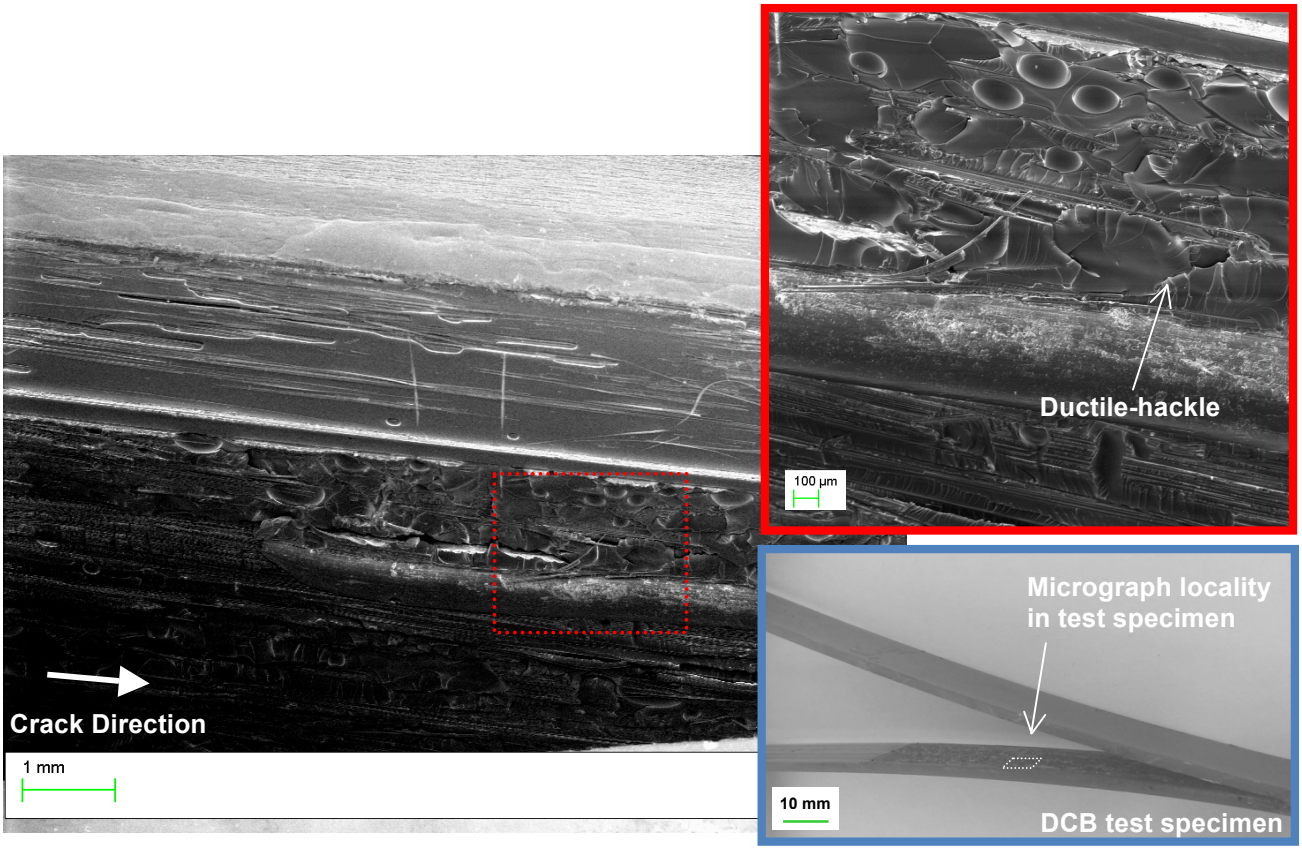

Figure 9. Microscopy investigation of the fracture plane for an E25 Sc (M) healed DCB specimen after re-test. Main image: Scanning electron micrograph (SEM) of the fracture plane. Lower inset image: Macro image of the DCB specimen indicating the position of the SEM image. Upper insert image: SEM of the fracture plane at higher magnification illustrating ductile-hackle features around loose glass fibres and the self-healed polymer (SHP).

Table 1. Specimen derivatives used to demonstrate self-healing performance.

Designation	Monomer Solution[a)]	Catalyst	Catalyst Loading [pph][b)]	Healing Temperature [°C]		
				45	80	RT
E10 Sc (M)	E10	$Sc(OTf)_3$	3.125 (M)	X	X	X
E10 Al (M)		$Al(OTf)_3$	3.125 (M)	X		
E25 Sc (M)	E25	$Sc(OTf)_3$	3.125 (M)	X	X	X
E25 Sc (H)			6.25 (H)	X		X
E25 Sc (L)			1.5625 (L)	X		
AUTO E25 Sc (M)			3.125 (M)	X		
E25 Al (M)		$Al(OTf)_3$	3.125 (M)	X		
E25 DETA		DETA	12			X

[a)] **E10**: 90 wt% EPON 828, 10 wt% Ethyl phenylacetate (EPA); **E25**: 75 wt% EPON 828, 25 wt% EPA. [b)] (L) = low loading, (M) = medium loading, (H) = high loading

Table 2. Glass transition temperatures (T_g) for self-healing polymers.

Designation	Healing Temperature [°C]	Glass transition temperature (T_g) [°C]
E10 Sc (M)	45	57
	80	63
	RT	51
E10 Al (M)	45	56
E25 Sc (M)	45	29
	80	48
	RT	28
E25 Sc (H)	45	46
	RT	21
E25 Sc (L)	45	23
E25 Al (M)	45	30
E25 DETA	RT	49

Table 3. DSC Data for E10 Metal Triflate Catalysts.

Designation	Heat of Reaction [J/g]	Onset Temperature [°C]	Maximum Temperature [°C]
E10 Sc (M)	337.9	34.6	129.2
E10 Al (M)	408.2	78.0	157.9
E10 Cu (M)	392.9	47.1	155.6

Table 4. Summary of G_{Ic} healing efficiencies

Designation	Initial G_{Ic} [J/m^2]	Healed G_{Ic} [J/m^2]	Healing Efficiency [%]	Healing Temperature [°C]
E10 Sc (M)	257 ± 23	307 ± 49	119 ± 15	45
	251 ± 13	279 ± 39	112 ± 20	80
	271 ± 22	228 ± 32	84 ± 10	RT
E10 Al (M)	215 ± 36	231 ± 62	109 ± 31	45
E25 Sc (M)	286 ± 9	571 ± 163	200 ± 53	45
	245 ± 24	743 ± 235	306 ± 103	80
	253 ± 12	308 ± 51	121 ± 19	RT
E25 Sc (H)	222 ± 18	780 ± 91	352 ± 38	45
	250 ± 18	459 ± 45	185 ± 24	RT
E25 Sc (L)	247 ± 19	433 ± 95	178 ± 50	45
AUTO E25 Sc (M)	241 ± 34	210 ± 63	88 ± 28	45
E25 Al (M)	232 ± 30	327 ± 90	141 ± 36	45
E25 DETA	218 ± 41	197 ± 52	95 ± 32	RT

The table of contents entry

An in-house developed Lewis acid-catalysed self-healing system, comprised of solid-phase metal triflate catalysts and diglycidyl ether bisphenol A (DGEBA) epoxy resin, is employed to achieve full fracture toughness recovery of the fibre reinforced polymer composite material. Mechanical testing of the healed material clearly shows a ductile failure, a failure mechanism not typically associated with inherently brittle materials such as epoxy.

Tim S. Coope, Duncan F. Wass, Richard S. Trask and Ian P. Bond*

Metal Triflates as Catalytic Curing Agents in Self-Healing Fibre Reinforced Composites

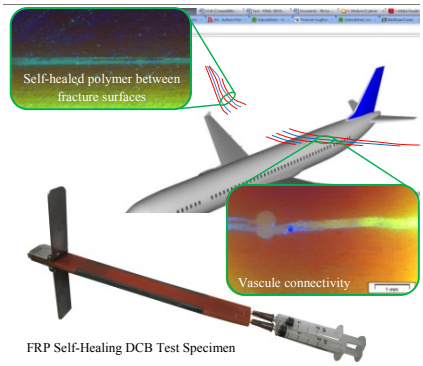

Copyright WILEY-VCH Verlag GmbH & Co. KGaA, 69469 Weinheim, Germany, 2011.

Supporting Information

for *Macromol. Mater. Eng.*, DOI: 10.1002/mame.201300026

Metal Triflates as Catalytic Curing Agents in Self-Healing Fibre Reinforced Composites

Tim S. Coope, Duncan F. Wass, Richard S. Trask and Ian P. Bond*

Table S1. DSC Data for $Sc(OTf)_3$ cured EPON 828

Designation	Heat of Reaction [J/g]	Onset Temperature [°C]	Maximum Temperature [°C]
EPON Sc (M)	464.7	81.6	199.3
E10 Sc (M)	337.9	34.6	129.2
E25 Sc (M)	280.4	49.8	143.2

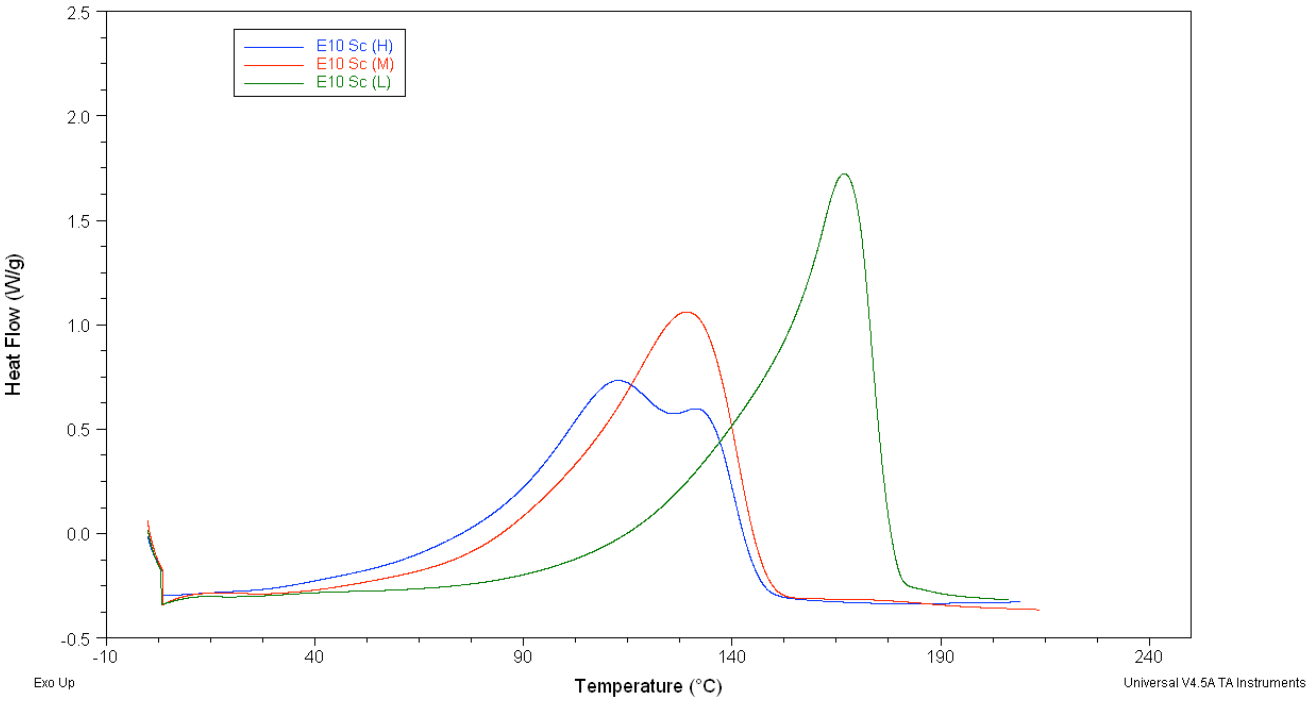

Figure S1. DSC curves for E10 Sc (H), E10 Sc (M) and E10 Sc (L) samples

Table S2. DSC Data for $Sc(OTf)_3$ cured EPON 828

Designation	Heat of Reaction [J/g]	Onset Temperature [°C]	Maximum Temperature [°C]
E10 Sc (L)	381.9	79.3	166.9
E10 Sc (M)	337.9	34.6	129.2
E10 Sc (H)	320.6	27.9	112.8

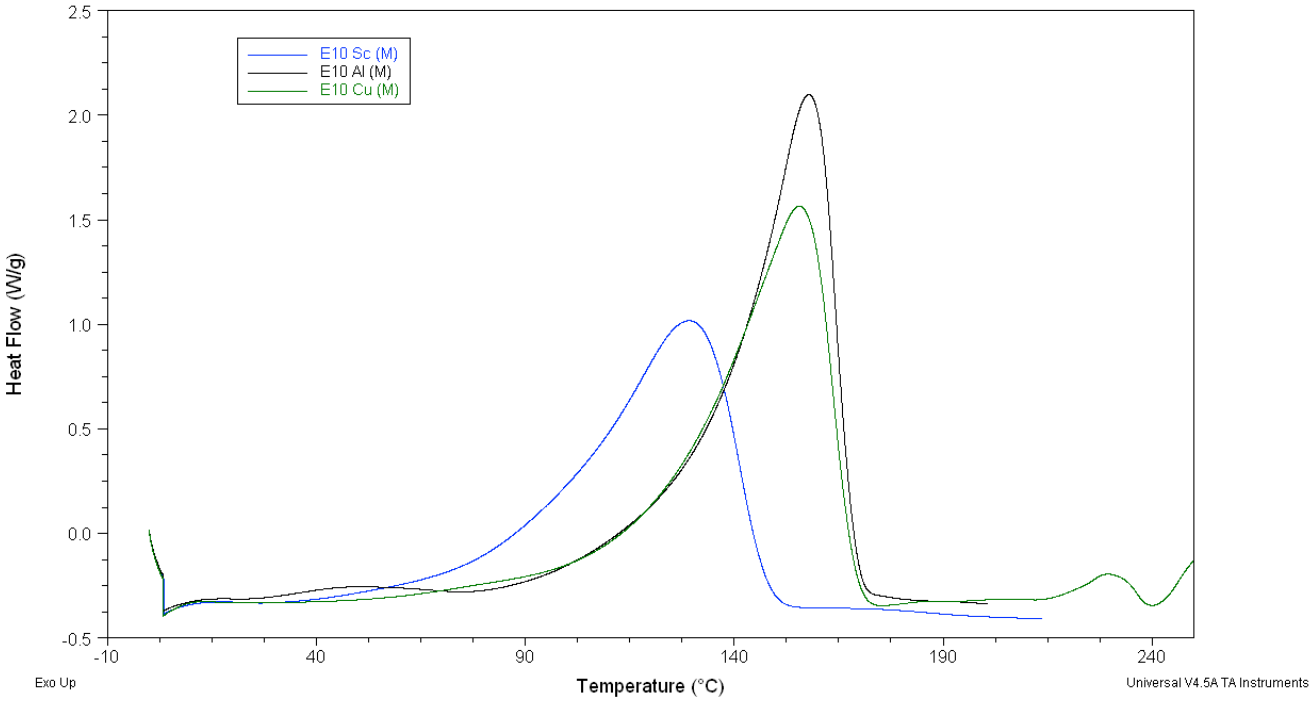

Figure S2. DSC curves for E10 Sc (M), E10 Al (M) and E10 Cu (M) samples

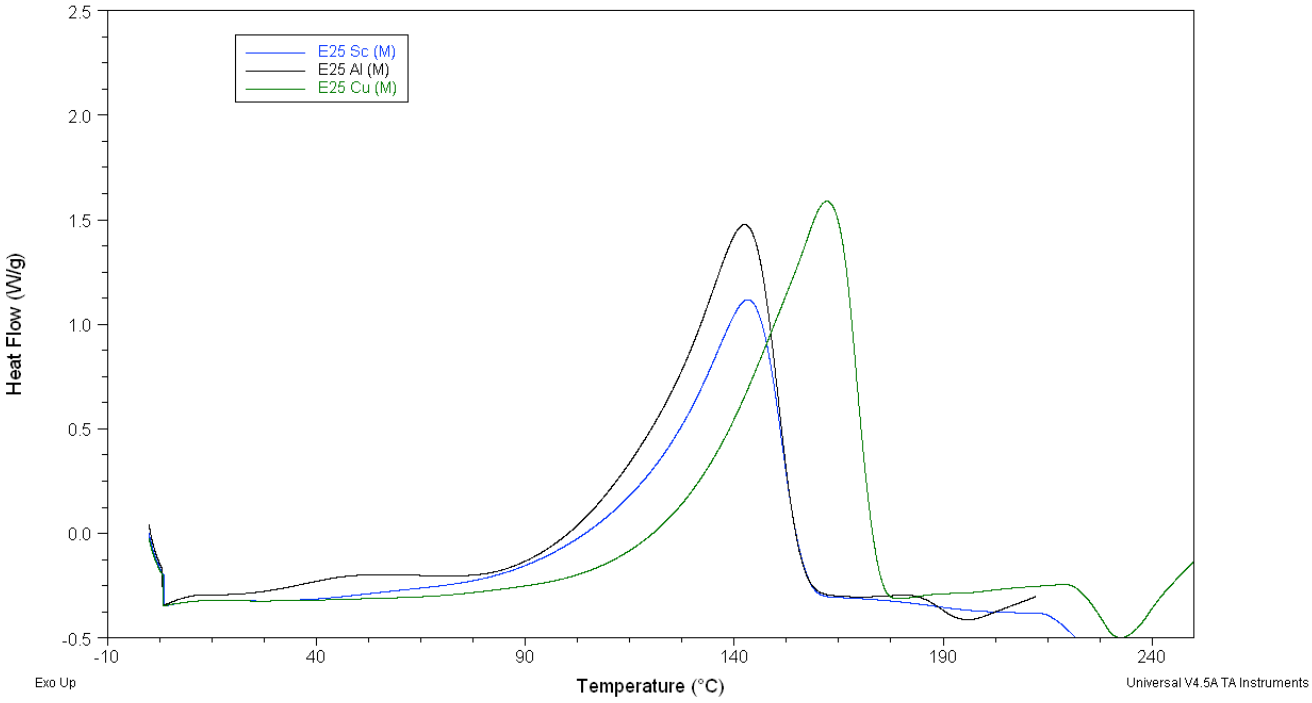

Figure S3. DSC curves for E25 Sc (M), E25 Al (M) and E25 Cu (M) samples

Table S3. DSC Data for Metal Triflate cured EPON 828

Designation	Heat of Reaction [J/g]	Onset Temperature [°C]	Maximum Temperature [°C]
E25 Sc (M)	280.4	49.8	143.2
E25 Al (M)	321.7	76.7	142.5
E25 Cu (M)	366.5	57.4	162.2

Self-Healed Polymer Testing:

Self-healed polymers (SHPs) were evaluated using a modified TDCB geometry to include a grooved short central trench (CT) section exclusively to contain the cured SHP.[9] SHP samples were prepared using precast CT sections, cured at 45 °C for 24 hours, with medium catalyst loading (Sc (M)). The precast SHP CT was placed in closed silicon moulds and the main geometry prepared from mixing 100 parts EPON 828 with 12 parts curing agent DETA into the prepared mould and left to cure for 24 hours at ambient temperature and 24 hours at 40 °C. A sharp razor blade was used to precrack cured samples prior to being pin-loaded on an Instron 3343 1 kN load cell at a displacement rate of 5 μm s^{-1}. Test specimens were cracked along the complete CT length until complete failure.

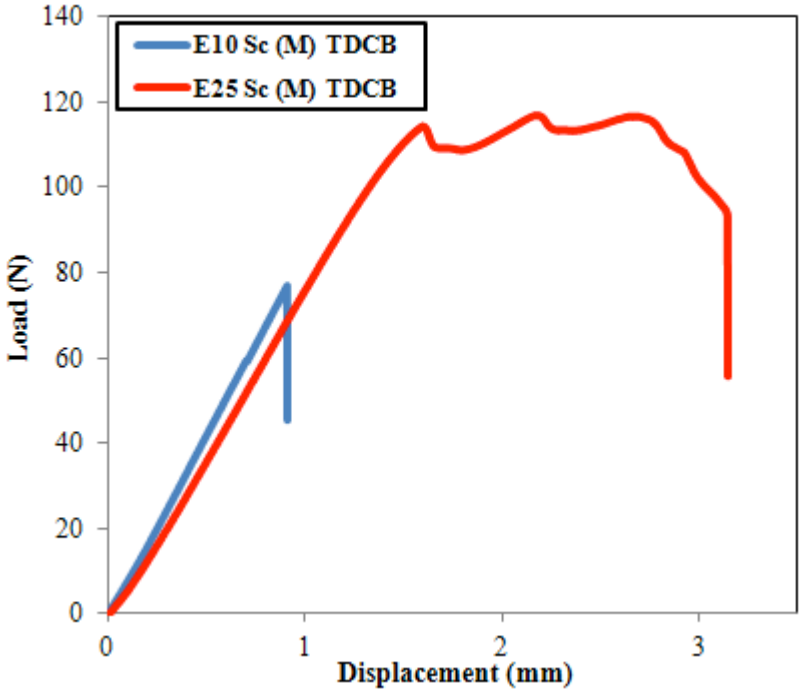

Figure S4. Representative load-displacement curve for initial fracture of E10 Sc (M) and E25 Sc (M) polymeric TDCB test specimens cured at 45 °C for 24 hours.

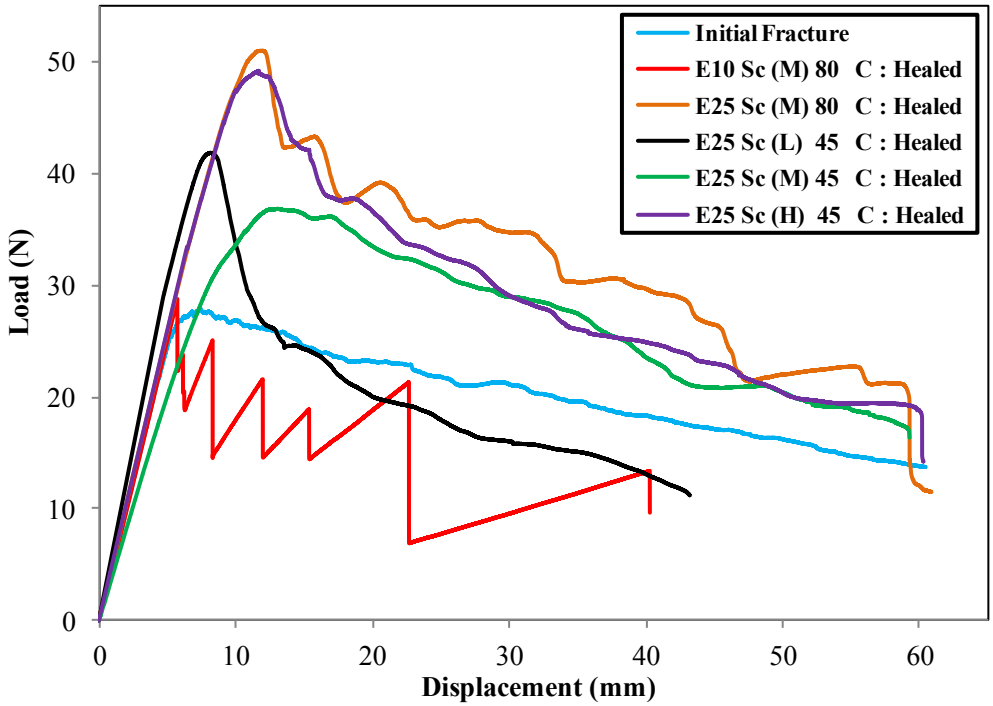

Figure S5. Representative load-displacement curves for $Sc(OTf)_3$ DCB test specimens healed at 45 °C and 80 °C for 24 hours.

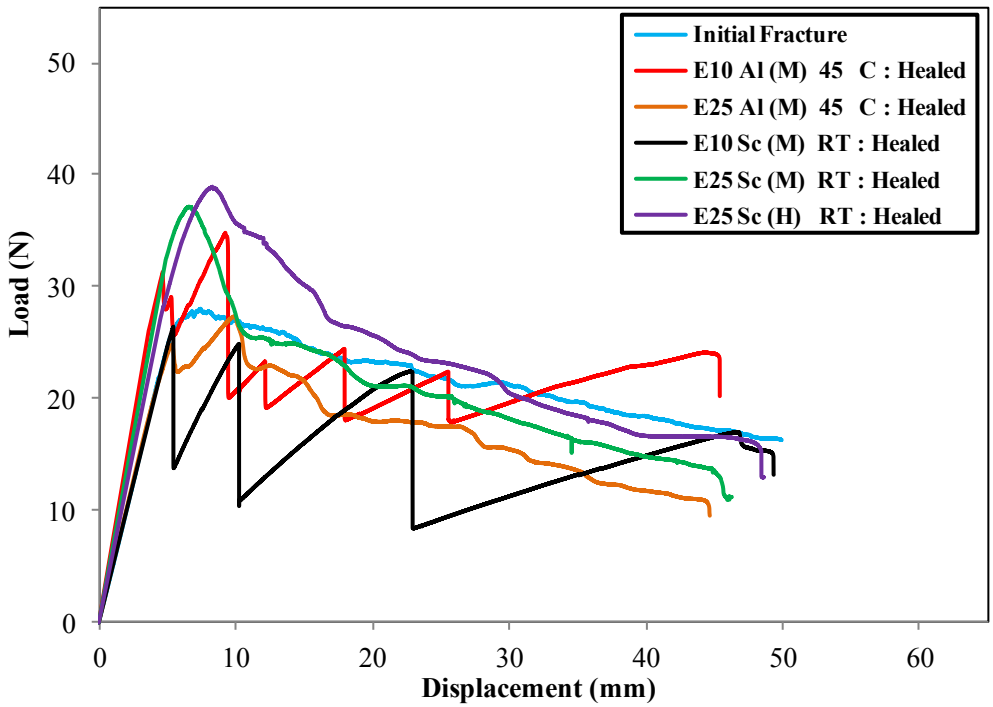

Figure S6. Representative load-displacement curves for $Al(OTf)_3$ DCB test specimens healed at 45 °C for 24 hours and $Sc(OTf)_3$ DCB test specimens healed at ambient temperature (RT) for 7 days.